IOPscience iopscience.iop.org

Home Search Collections Journals About Contact us My IOPscience

Conductometric chemical sensor based on individual CuO nanowires

This article has been downloaded from IOPscience. Please scroll down to see the full text article.

2010 Nanotechnology 21 485502

(http://iopscience.iop.org/0957-4484/21/48/485502)

View the table of contents for this issue, or go to the journal homepage for more

Download details:
IP Address: 169.234.66.208
The article was downloaded on 31/12/2012 at 06:01

Please note that terms and conditions apply.

Nanotechnology **21** (2010) 485502 (6pp) doi:10.1088/0957-4484/21/48/485502

Conductometric chemical sensor based on individual CuO nanowires

Dongdong Li[1,2], Jun Hu[3], Ruqian Wu[3] and Jia G Lu[2,4]

[1] Division of Energy and Environmental Research, Shanghai Advanced Research Institute, Chinese Academy of Sciences, Shanghai 201203, People's Republic of China
[2] Department of Physics and Department of Electrical Engineering, University of Southern California, Los Angeles, CA 90089-0484, USA
[3] Department of Physics and Astronomy, University of California, Irvine, Irvine, CA 92697-4575, USA

E-mail: jia.grace.lu@usc.edu

Received 8 July 2010, in final form 17 October 2010
Published 4 November 2010
Online at stacks.iop.org/Nano/21/485502

Abstract
CuO nanowires with high crystalline quality are synthesized via a simple thermal oxidation method. Charge conduction on individual nanowires under a transverse electric field exhibits an intrinsic p-type semiconducting behavior. Variations in signal transducer in different chemical gas environments are measured on individual CuO nanowire field effect transistors. They demonstrate good performance to both NO_2 and ethanol gasses. In particular, the nanowire chemical sensor reveals a reverse response to ethanol vapor under temperature variation. Experimental results and first-principles calculations indicate that ethanol is oxidized in air at high temperature, resulting in the production of CO_2 and H_2O. The strong H_2O adsorption leads to the reversal behavior, due to the electron transfer from H_2O molecules to the CuO surface.

(Some figures in this article are in colour only in the electronic version)

1. Introduction

Cupric oxide (CuO), with a bandgap of 1.0–1.9 eV [1–5], is intrinsically a p-type semiconductor mainly due to the Cu vacancies [1]. Many methods have been developed for the synthesis of CuO nanostructures [2–7], and the vapor–solid oxidation approach has been demonstrated to be particularly useful for the growth of vertically aligned CuO nanowires (NWs) with high crystalline quality [7, 8]. Due to their high aspect ratio and large surface-to-volume ratio, quasi-one-dimensional (Q1D) nanostructured CuO has high sensitivity to the change of environment and enhanced chemical activity towards adsorbates. CuO NWs hence have been extensively investigated for various applications as lithium–copper oxide electrochemical cells [9], fuel cells [10], solar cells [11], nanocatalysts [12], field emission emitters [11, 13] and gas sensors [4–6, 14, 15]. Recent studies focused on their electrical properties, especially the effect of surface adsorption on carrier conduction through oxide nanowires [16]. It is imperative to further develop efficient nanodevices, based on a clear understanding from experimental explorations. Herein, the electrical transport and chemical gas sensing properties are presented on individual CuO nanowires that are configured as field effect transistors. The sensing mechanism with various target gases is then quantitatively investigated by combining first-principles calculations and experimental findings.

[4] Author to whom any correspondence should be addressed.

2. Synthesis and material characterization

CuO nanowires are vertically grown under thermal oxidation of Cu foils in a furnace at 600 °C for 6 h in static air. In the oxidation process, a dense Cu_2O film is first formed on the Cu foil ($Cu + O_2 \rightarrow Cu_2O$). CuO nanowires ($Cu_2O + O_2 \rightarrow CuO$) are then produced on the top layer following complete oxidation [7].

Figure 1(a) shows the scanning electron micrograph (SEM) images of CuO nanowires with diameters ranging from 30 to 100 nm. The x-ray diffraction pattern (figure 1(b)) of the as-synthesized film can be indexed as monoclinic CuO (JCPDS file no. 45-0937) nanowires and the underlayered cubic Cu_2O (JCPDS file no. 05-0667) film. In our experiment, both single-crystal and bicrystal CuO nanowires are observed via transmission electron microscopy (TEM)

 © 2010 IOP Publishing Ltd Printed in the UK & the USA

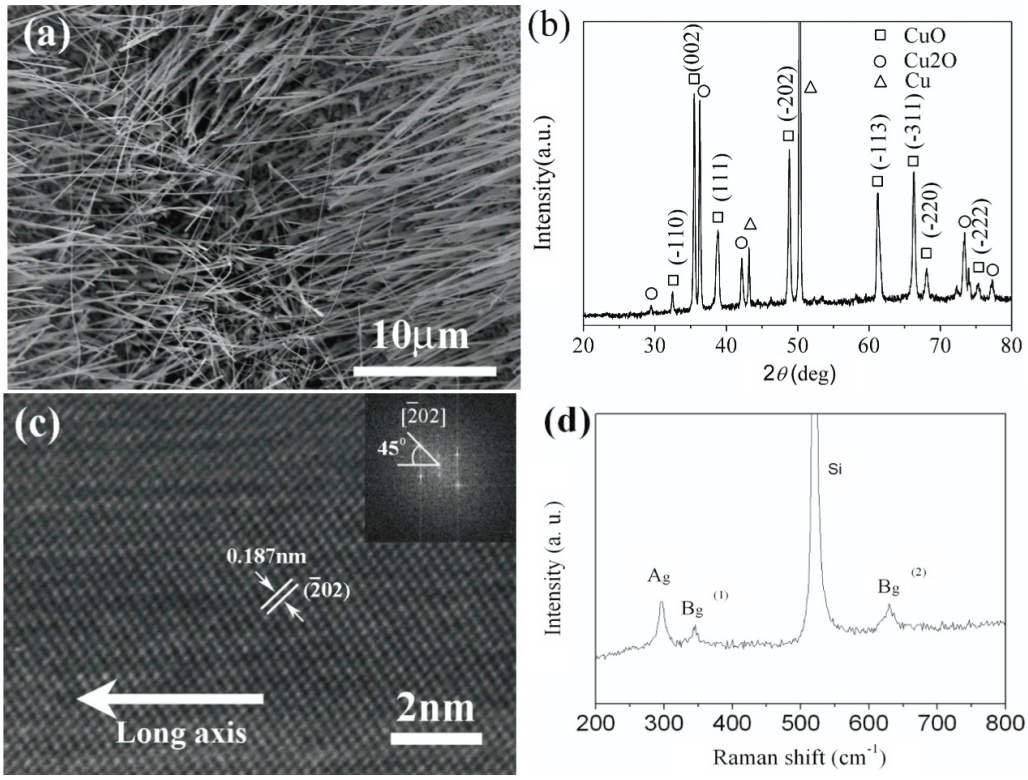

Figure 1. (a) An SEM image of free-standing CuO nanowire arrays. (b) XRD pattern of as-obtained film indicates the existence of monoclinic CuO and cubic Cu_2O. (c) HRTEM image and the corresponding FFT image (inset) of a CuO nanowire. (d) Micro-Raman spectrum for an individual CuO nanowire.

analysis. Figure 1(c) and the inset display a high-resolution TEM image of a single-crystal CuO nanowire and the corresponding fast Fourier transform (FFT) analysis. The interplanar spacing of 0.187 nm can be indexed to the ($\bar{2}$02) planes, indicating a ∼45° angle between the [$\bar{2}$02] direction and the wire long axis. Figure 1(d) represents the micro-Raman spectrum of an individual nanowire on the Si substrate. The measurement is carried out at ambient conditions with a 532 nm wavelength laser excitation. The three strong peaks (297, 345 and 632 cm^{-1}) indicate that the three main phonon modes in the CuO crystal corresponding to the three Raman-active modes of A_g, $B_g^{(1)}$ and $B_g^{(2)}$ symmetries [17].

The as-synthesized CuO nanowires are suspended in isopropyl alcohol, and then pipette-deposited onto degenerately doped Si substrates capped with a 500 nm SiO_2 layer at a controllable density. Photolithography followed by drain (D) and source (S) electrode deposition of Ti (5 nm)/Au (50 nm) are conducted to define contact patterns with 2 μm inter-electrode distance. Figure 2(a) plots the current–voltage (I_{DS}–V_{DS}) curves of an individual CuO nanowire field effect transistor (NWFET) measured at room temperature under different gate voltages (from −80 to 80 V), presenting p-type behavior with weak gate dependence. The nonlinear I_{DS}–V_{DS} curves arise from the Schottky barrier due to the small work function of Ti (∼4.33 eV) compared to that of the p-type CuO (∼4.50 eV) [18]. The conductivity extracted from the linear region of I_{DS}–V_{DS} curve is around 1.1×10^{-3} S cm^{-1}, based on a cylindrical wire geometry with a diameter of ∼80 nm. The conductivity is higher than that of polycrystalline nanowires because of reduced scattering along the crystalline wires [3]. Note that this is still a lower bound of the intrinsic conductivity value since the two-probe measurement cannot separate out the electrode contact resistances. The nanowire device reveals a small transconductance ($g_m = \mathrm{d}I_{DS}/\mathrm{d}V_g \sim 3.84 \times 10^{-11}$ S), which is calculated from the linear slope under a bias voltage (V_{DS}) of 10 V, as displayed in the I_{DS}–V_g curve (figure 2(b)).

The back gate capacitance for this Q1D system can be estimated as $C = \frac{2\pi\varepsilon_0\varepsilon_r L}{\ln(4h/d)}$, where L is the length of the nanowire channel, ε_r (∼2.66) the effective dielectric constant of the gate (estimated as the average value of dielectric constants of vacuum and the bulk SiO_2, $\varepsilon_{SiO2} = 3.9$) [19], h the thickness of the SiO_2 film and d the diameter of CuO nanowire. The field effect mobility and carrier concentration are estimated to be $\mu = 2.51 \times 10^{-3}$ cm^2 V^{-1} s^{-1} and $n = 9.04 \times 10^{19}$ cm^{-3} using the following expressions: $\mu = \frac{g_m L^2}{C V_{DS}}$ and $n = \frac{V_g(\mathrm{th})}{e} \times \frac{C}{L}$, where V_g(th) is extrapolated along the slope of the transconductance curve [20].

The I_{DS}–V_{DS} curves plotted in figure 2(c) illustrate an increase in conductivity with temperature. Figure 2(d) shows the semi-logarithmic graph of conductivity versus reciprocal temperature for the CuO nanowire exposed to air, ethanol (0.37% mixed with air) and NO_2 (50 ppm mixed with Ar), respectively. The linear fit indicates Arrhenius-type behavior following the expression of $\sigma \propto e^{-Ea/kT}$, where E_a, k (=8.617×10^{-5} eV K^{-1}) and T are the activation energy, Boltzmann constant and absolute temperature [21]. The values

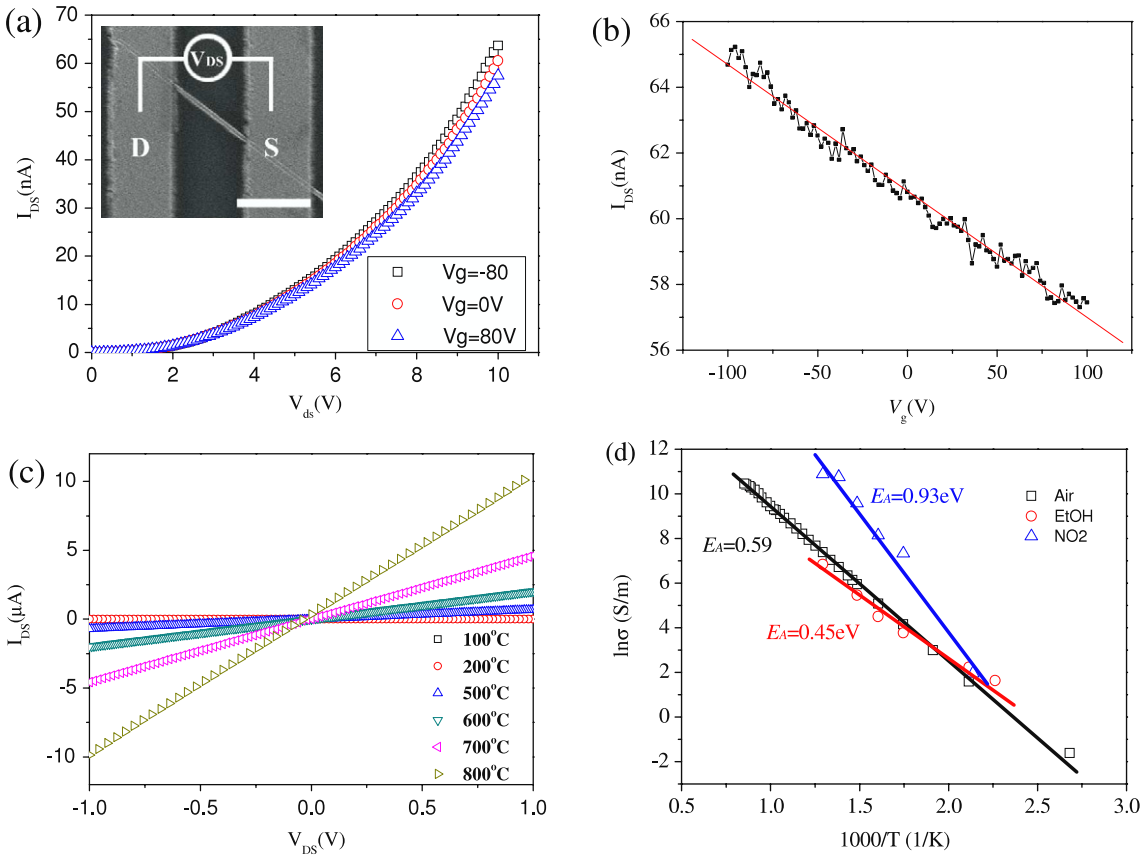

Figure 2. (a) Typical I_{DS}–V_{DS} characteristics of an individual CuO nanowire for different gate biases from −80 to 80 V. Inset: an SEM image for the nanowire connected with drain (D) and source (S) electrodes; the scale bar is 2 μm long. (b) The transconductance (I_{DS}–V_g) curve at $V_{DS} = 10$ V. (c) The I_{ds}–V_{ds} curves of an individual nanowire measured at different temperatures: 100, 200, 500, 600, 700 and 800 °C, respectively. (d) A semi-logarithmic plot of conductivity (σ) versus reciprocal temperature ($1/T$) in air, ethanol (0.37% mixed with air) and NO_2 (50 ppm mixed with Ar).

of E_a extracted from the slopes in figure 2(d) are 0.59 eV (air), 0.45 eV (ethanol + air) and 0.93 eV (NO_2), respectively. Note that, upon adsorption on the p-type nanowire surface, the NO_2 molecules act as hole donors, consequently the conductivity of the nanowire is increased. To elucidate the temperature dependence of conductivity, the NO_2 gas is mixed with an inert gas (Ar). On the other hand, the ethanol sensing is generally based on the reaction of reducing gas (i.e. ethanol) and the pre-existing surface adsorbed oxygen. Thus, air is employed as the carrier gas in ethanol sensing.

Gas sensing properties are characterized for an individual nanowire ($V_{DS} = 1$ V) in a quartz chamber with electrical feedthrough [22]. Because of the high surface-to-volume ratio (proportional to $1/r$) [23] and small radius comparable to the Debye length, the surface effect is very pronounced in Q1D structured sensors. Figure 3(a) depicts the reproducible sensing response during four adsorption–desorption cycles by switching from air ambient pressure to vacuum (300 mTorr) at 350 °C. The desorption of O_2 molecules under low pressure suppresses conductivity, due to the p-type nature of the CuO channel. However the response time is not evaluated because of the pumping process. Figure 3(b) plots the sensing characteristic of an individual CuO nanowire towards an NO_2 pulse mixed with Ar at 350 °C. Here we define the gas response as $S = (G - G_0)/G_0$, where G_0 and G are the respective conductances before and after the gas exposure; and response time as the time that is needed to reach $1/e$ of the saturation status after the exposure to the target gas. It is observed that a 12.5 ppm NO_2 pulse results in a 9% conduction increase with a response time of about 50 s. The inset presents the absolute value of gas response versus NO_2 concentration. The performance is comparable to the sensor of CuO 'nanoplates' pasted on a ceramic tube [24].

When sensing of CuO is conducted under ethanol pulses using air as carrier gas, it is observed that the conductance increases rapidly when exposed to the ethanol vapor under 170 °C: 0.37% ethanol leads to ∼70% conductivity rise with a response time of ∼27 s (figure 3(c)). In contrast, a reversal in conductance change occurs when temperature rises. As shown in figure 3(d), at 500 °C, 0.37% ethanol vapor leads to ∼70% conductivity reduction with a response time of ∼40 s. Similarly, 0.13% ethanol vapor causes ∼42% conduction decrease with the response time of ∼70 s. The inset shows the concentration dependence of sensitivity in absolute value.

3. Simulation results

To explore the microscopic mechanism behind our experimental results given above, density functional calculations of molecular adsorptions on monoclinic CuO crystal surfaces

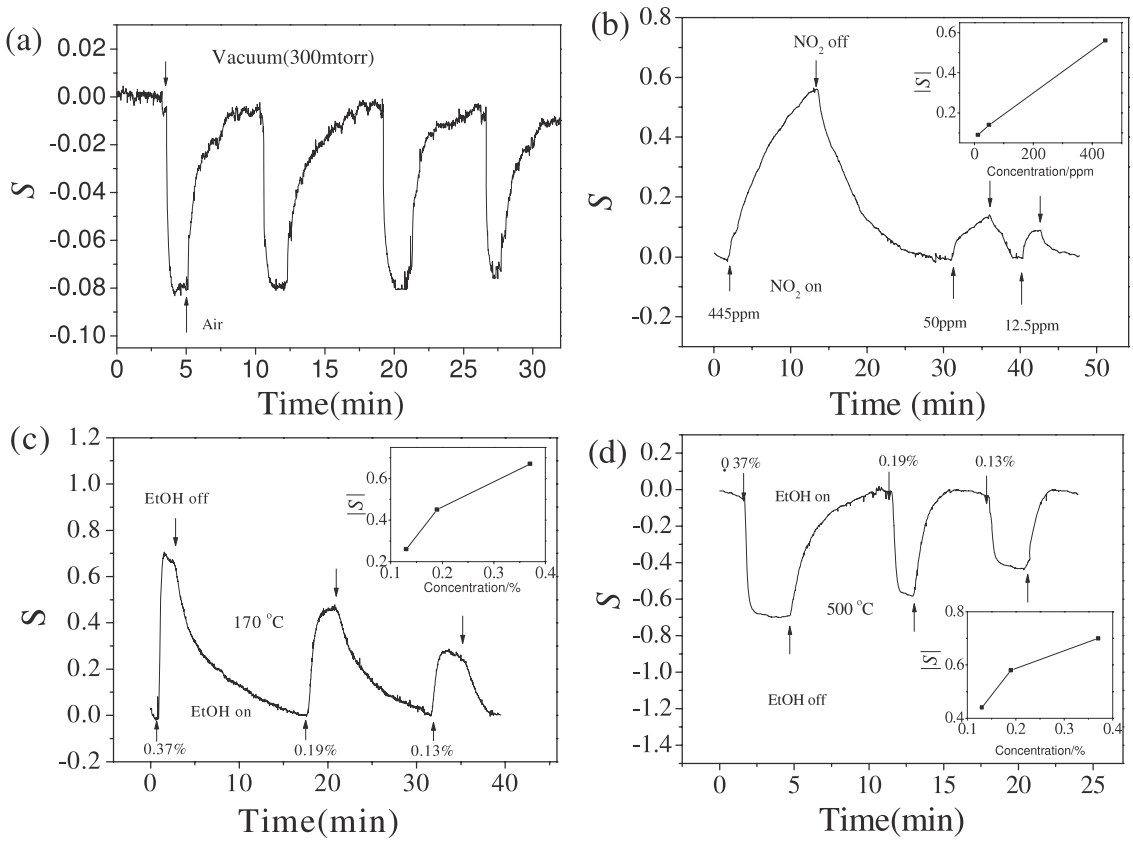

Figure 3. Gas responses (a) by switching vacuum (300 mTorr) and atmospheric pressure at 350 °C, (b) and to NO_2 gas at different concentration at 350 °C. Gas responses to diluted ethanol gas mixed with air measured at (c) 170 °C and (d) 500 °C, respectively. The bias voltage on nanowire is 1 V. Insets of (b)–(d) represent the concentration dependence of $|S|$.

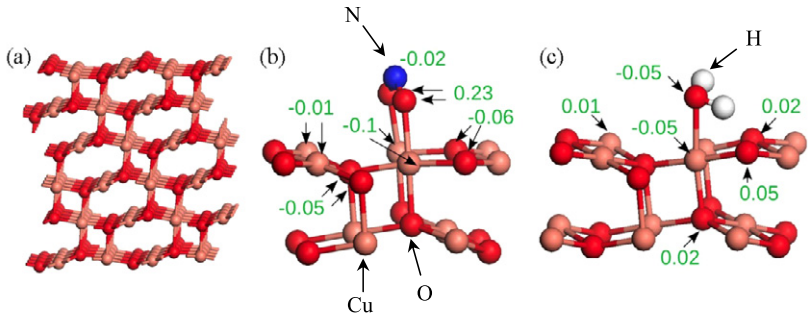

Figure 4. (a) Structural model of CuO(111). (b) and (c) adsorption geometries and charge transfers of NO_2 and H_2O molecules on the CuO(111) surface. The salmon pink, red, blue and gray balls represent Cu, O, N and H atoms, respectively.

are carried out with the Vienna *ab initio* simulation package (VASP) [25, 26] using the projector augmented wave (PAW) method [27, 28] and the generalized-gradient approximation (GGA) [29]. In order to properly describe the strong correlation effect in CuO, we invoke a Hubbard U correction [30], with parameters (U and J) taken from the literature [1]. The plane-wave cutoff energy is set to be 400 eV.

Here we simply consider molecular adsorptions on the CuO(111) surface as displayed in figure 4(a), since it is the most stable surface of CuO [31]. For both NO_2 and ethanol adsorptions, the O atoms in adsorbates favor to bind to the surface Cu atom (denoted as Cu_s), with Cu_s–O bond lengths of 1.98 and 2.10 Å, respectively. For O_2 adsorption, one of the O atoms interacts with Cu_s, with a Cu_s–O bond length of 1.98 Å, whereas the other atom remains away from the surface. The binding energies (E_b) of NO_2, ethanol and O_2 adsorptions are 0.96, 0.44 and 0.27 eV, respectively.

The charge transfer between chemical gas molecules and the sensor material governs the sensing principle of a conductometric chemical sensor [23, 32, 33]. When an oxidizing gas is introduced, the conductivity of a p-type semiconductor increases due to the transfer of electrons to adsorbates and thereby the increase of hole carrier concentration in CuO [4, 6]. We found sizable electron transfer from the CuO surface to NO_2 as shown in figure 4(b). Each oxygen atom of NO_2 receives 0.23 electrons, while the N atom

loses 0.02 electrons according to Bader charge analysis. Thus the CuO surface totally loses 0.44 electrons to each NO_2 molecule and an accumulation layer forms on the p-type nanowire surface. This results in the conductance increase as shown in figure 3(b). Likewise the adsorption of one O_2 molecule draws 0.19 electrons from the CuO(111) surface, presenting similar conductance response to NO_2 gas. One can hence conclude the removal of O_2 in vacuum as the key reason for the reduction of conductance as plotted in figure 3(a).

The temperature-dependent response of CuO nanowires to ethanol gas is more complex. As we know, ethanol reacts with O_2 at high temperature (i.e. 500 °C), forming CO_2 and H_2O ($C_2H_5OH + 3O_2 \rightarrow 2CO_2 + 3H_2O$). We found that the CO_2 molecule can hardly adsorb on the CuO(111) surface so that it does not affect the conductance. In contrast, the interaction between H_2O and CuO(111) is very strong, with E_b of 1.37 eV. This means that the H_2O molecule can tightly bond on the CuO(111) surface even at high temperature. Figure 4(c) illustrates the charge transfer between CuO(111) and H_2O, where 0.02 extra electrons are transferred from each H_2O molecule to the CuO surface. Since the coverage of H_2O is high due to the large E_b, the hole concentration and hence the conductance are subsequently reduced. At low temperature (i.e. 170 °C), no obvious charge transfer between ethanol and CuO(111) was found in our calculations. The conductance increase observed at 170 °C may associate with ethanol adsorption on other facets, the effect of Cu vacancies, or indirect factors such as the facilitation of extra O_2 adsorption on CuO nanowires.

4. Conclusions

CuO nanowires are obtained by direct sintering Cu foil in static air and their electrical transport properties investigated in a FET geometry. The conductivity, charge concentration and field effect mobility are estimated to be $\sim 1.1 \times 10^{-3}$ S cm^{-1}, 9.04×10^{19} cm^{-3} and 2.51×10^{-3} cm^2 V^{-1} s^{-1}, respectively. The gas sensing response based on the CuO nanowire conductometric sensors are carried out in air, NO_2 and ethanol. The air and NO_2 pulses lead to a conductance increase, while a reverse response in ethanol vapor at different temperatures is observed. First-principles calculations of molecular adsorption on CuO surfaces indicate that the adsorptions of NO_2 and O_2 draw electrons out of CuO and increase conductance. Under high temperature, ethanol reacts with O_2 in the carrier gas to split into CO_2 and H_2O. The H_2O adsorption is dominant on the CuO surface due to the strong binding energy. Additionally, H_2O molecules donate electrons to CuO and lead to a reduction of conductance. The insights developed here are useful for the integration of various nanowire sensors (p-type CuO and n-type ZnO, SnO_2 and In_2O_3) for potential 'nanoelectronic nose' devices for detecting complex gas mixtures.

Acknowledgments

Work in USC was supported by a DOE EFRC grant. Work in UCI was supported by DOE grant DE-FG02-05ER46237. The authors thank Drs Paichun Chang and PoChiang Chen for their valuable suggestions in the sensing experiment.

References

[1] Wu D, Zhang Q and Tao M 2006 LSDA + U study of cupric oxide: electronic structure and native point defects *Phys. Rev.* B **73** 235206
[2] Wang W, Liu Z, Liu Y, Xu C, Zheng C and Wang G 2003 A simple wet-chemical synthesis and characterization of CuO nanorods *Appl. Phys.* A **76** 417–20
[3] Wu H, Lin D D and Pan W 2006 Fabrication, assembly, and electrical characterization of CuO nanofibers *Appl. Phys. Lett.* **89** 133125
[4] Gou X L, Wang G X, Yang J S, Park J and Wexler D 2008 Chemical synthesis, characterisation and gas sensing performance of copper oxide nanoribbons *J. Mater. Chem.* **18** 965–9
[5] Zhang J T, Liu J F, Peng Q, Wang X and Li Y D 2006 Nearly monodisperse Cu_2O and CuO nanospheres: preparation and applications for sensitive gas sensors *Chem. Mater.* **18** 867–71
[6] Wang C, Fu X Q, Xue X Y, Wang Y G and Wang T H 2007 Surface accumulation conduction controlled sensing characteristic of p-type CuO nanorods induced by oxygen adsorption *Nanotechnology* **18** 145506
[7] Jiang X C, Herricks T and Xia Y N 2002 CuO nanowires can be synthesized by heating copper substrates in air *Nano Lett.* **2** 1333–8
[8] Hsieh C T, Chen J M, Lin H H and Shih H C 2003 Synthesis of well-ordered CuO nanofibers by a self-catalytic growth mechanism *Appl. Phys. Lett.* **82** 3316–8
[9] Wang S Q, Zhang J Y and Chen C H 2007 Dandelion-like hollow microspheres of CuO as anode material for lithium-ion batteries *Scr. Mater.* **57** 337–40
[10] Chang C L, Hsu C C and Huang T J 2003 Cathode performance and oxygen-ion transport mechanism of copper oxide for solid-oxide fuel cells *J. Solid State Electrochem.* **7** 125–8
[11] Liu Y L, Liao L, Li J C and Pan C X 2007 From copper nanocrystalline to CuO nanoneedle array: synthesis, growth mechanism, and properties *J. Phys. Chem.* C **111** 5050–6
[12] Reitz J B and Solomon E I 1998 Propylene oxidation on copper oxide surfaces: electronic and geometric contributions to reactivity and selectivity *J. Am. Chem. Soc.* **120** 11467–78
[13] Zhu Y W, Yu T, Cheong F C, Xui X J, Lim C T, Tan V B C, Thong J T L and Sow C H 2005 Large-scale synthesis and field emission properties of vertically oriented CuO nanowire films *Nanotechnology* **16** 88–92
[14] Raksa P, Gardchareon A, Chairuangsri T, Mangkorntong P, Mangkorntong N and Choopun S 2009 Ethanol sensing properties of CuO nanowires prepared by an oxidation reaction *Ceram. Int.* **35** 649–52
[15] Hansen B J, Kouklin N, Lu G H, Lin I K, Chen J H and Zhang X 2010 Transport, analyte detection, and opto-electronic response of p-type CuO nanowires *J. Phys. Chem.* C **114** 2440–7
[16] Kolmakov A and Moskovits M 2004 Chemical sensing and catalysis by one-dimensional metal-oxide nanostructures *Annu. Rev. Mater. Res.* **34** 151–80
[17] Chrzanowski J and Irwin J C 1989 Raman-scattering from cupric oxide *Solid State Commun.* **70** 11–4
[18] Zhu Y W *et al* 2006 Enhanced field emission from O-2 and CF4 plasma-treated CuO nanowires *Chem. Phys. Lett.* **419** 458–63
[19] Thompson R S, Li D, Witte C M and Lu J G 2009 Weak localization and electron–electron interactions in indium-doped ZnO nanowires *Nano Lett.* **9** 3991–5
[20] Martel R, Schmidt T, Shea H R, Hertel T and Avouris P 1998 Single- and multi-wall carbon nanotube field-effect transistors *Appl. Phys. Lett.* **73** 2447–9

[21] Chang P C and Lu J G 2008 Temperature dependent conduction and UV induced metal-to-insulator transition in ZnO nanowires *Appl. Phys. Lett.* **92** 212113
[22] Fan Z Y and Lu J G 2005 Gate-refreshable nanowire chemical sensors *Appl. Phys. Lett.* **86** 123510
[23] Fan Z Y and Lu J G 2006 Chemical sensing with ZnO nanowire field-effect transistor *IEEE Trans. Nanotechnol.* **5** 393–6
[24] Li Y M, Liang J, Tao Z H and Chen J 2008 CuO particles and plates: synthesis and gas-sensor application *Mater. Res. Bull.* **43** 2380–5
[25] Kresse G and Furthmuller J 1996 Efficiency of *ab initio* total energy calculations for metals and semiconductors using a plane-wave basis set *Comput. Mater. Sci.* **6** 15–50
[26] Kresse G and Furthmuller J 1996 Efficient iterative schemes for *ab initio* total-energy calculations using a plane-wave basis set *Phys. Rev.* B **54** 11169–86
[27] Blochl P E 1994 Projector augmented-wave method *Phys. Rev.* B **50** 17953–79
[28] Kresse G and Joubert D 1999 From ultrasoft pseudopotentials to the projector augmented-wave method *Phys. Rev.* B **59** 1758–75
[29] Perdew J P 1991 *Electronic Structure of Solids '91* (Berlin: Akademie)
[30] Dudarev S L, Botton G A, Savrasov S Y, Humphreys C J and Sutton A P 1998 Electron-energy-loss spectra and the structural stability of nickel oxide: an LSDA + U study *Phys. Rev.* B **57** 1505–9
[31] Hu J, Li D, Lu J G and Wu R 2010 Effects on electronic properties of molecule adsorption on CuO surface and nanowire *J. Phys. Chem.* C **114** 17120–6
[32] Sysoev V V, Goschnick J, Schneider T, Strelcov E and Kolmakov A 2007 A gradient microarray electronic nose based on percolating SnO_2 nanowire sensing elements *Nano Lett.* **7** 3182–8
[33] Henrich V E and Cox P A 1994 *The Surface Science of Metal Oxides* (Cambridge: Cambridge University Press)